

NO-A143 041

SATURN'S RINGS: 3-MM LOW-INCLINATION OBSERVATIONS AND
DERIVED PROPERTIES.. (U) AEROSPACE CORP EL SEGUNDO CA
ELECTRONICS RESEARCH LAB E E EPSTEIN ET AL. 15 JUN 84

1/1

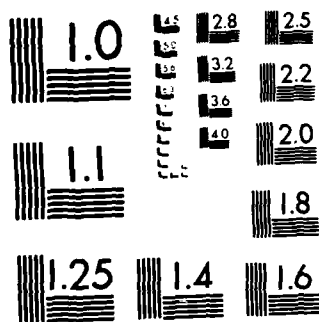
UNCLASSIFIED

TR-0004(4925-06)-3 SD-TR-84-23

F/G 3/2

ML





MICROCOPY RESOLUTION TEST CHART
NATIONAL BUREAU OF STANDARDS-1963-A

12

Saturn's Rings: 3-mm Low-Inclination Observations and Derived Properties

AD-A143 841

E. E. EPSTEIN
✓ Electronics Research Laboratory
Laboratory Operations
The Aerospace Corporation
El Segundo, Calif. 90245

M. A. JANSSEN
Jet Propulsion Laboratory
California Institute of Technology
Pasadena, Calif. 91103

J. N. CUZZI
Ames Research Center
National Aeronautics and Space Administration
Moffett Field, Calif. 94035

15 June 1984

APPROVED FOR PUBLIC RELEASE;
DISTRIBUTION UNLIMITED

400 34
E

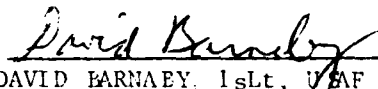
ENC FILE COPY

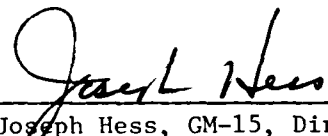
Prepared for
SPACE DIVISION
AIR FORCE SYSTEMS COMMAND
Los Angeles Air Force Station
P.O. Box 92960, Worldway Postal Center
Los Angeles, Calif. 90009

This report was submitted by The Aerospace Corporation, El Segundo, CA 90245, under Contract No. F04701-83-C-0084 with the Space Division, P.O. Box 92960, Worldway Postal Center, Los Angeles, CA 90009. It was reviewed and approved for The Aerospace Corporation by D. H. Phillips, Director, Electronics Research Laboratory. First Lt David Barnaby, SD/YNCS, was the Project Officer for the Mission Oriented Investigation and Experimentation (MOIE) Program.

This report has been reviewed by the Public Affairs Office (PAS) and is releasable to the National Technical Information Service (NTIS). At NTIS, it will be available to the general public, including foreign nationals.

This technical report has been reviewed and is approved for publication. Publication of this report does not constitute Air Force approval of the report's findings or conclusions. It is published only for the exchange and stimulation of ideas.


DAVID BARNAEY, 1st Lt, USAF
Monitor, Mission Oriented Investigation
and Experimentation Program


Joseph Hess, GM-15, Director, West Coast
Office, AF Space Technology Center

UNCLASSIFIED

SECURITY CLASSIFICATION OF THIS PAGE (When Data Entered)

REPORT DOCUMENTATION PAGE		READ INSTRUCTIONS BEFORE COMPLETING FORM
1. REPORT NUMBER SD-TR-84-23	2. GOVT ACCESSION NO. <i>A143 841</i>	3. RECIPIENT'S CATALOG NUMBER
4. TITLE (and Subtitle) SATURN'S RINGS: 3-mm LOW-INCLINATION OBSERVATIONS AND DERIVED PROPERTIES		5. TYPE OF REPORT & PERIOD COVERED
		6. PERFORMING ORG. REPORT NUMBER TR-0084(4925-06)-3
7. AUTHOR(s) Eugene E. Epstein, Michael A. Janssen, and Jeffrey N. Cuzzi		8. CONTRACT OR GRANT NUMBER(s) F04701-83-C-0084
9. PERFORMING ORGANIZATION NAME AND ADDRESS The Aerospace Corporation El Segundo, Calif. 90245		10. PROGRAM ELEMENT, PROJECT, TASK AREA & WORK UNIT NUMBERS
11. CONTROLLING OFFICE NAME AND ADDRESS Space Division Air Force Systems Command Los Angeles, Calif. 90009		12. REPORT DATE 15 June 1984
		13. NUMBER OF PAGES 29
14. MONITORING AGENCY NAME & ADDRESS (if different from Controlling Office)		15. SECURITY CLASS. (of this report) Unclassified
		15a. DECLASSIFICATION/DOWNGRADING SCHEDULE
16. DISTRIBUTION STATEMENT (of this Report) Approved for public release; distribution unlimited.		
17. DISTRIBUTION STATEMENT (of the abstract entered in Block 20, if different from Report)		
18. SUPPLEMENTARY NOTES		
19. KEY WORDS (Continue on reverse side if necessary and identify by block number) Rings of Saturn: Millimeter-Wave Observations Rings of Saturn: Particle Size Distribution and Composition		
20. ABSTRACT (Continue on reverse side if necessary and identify by block number) We have combined recent 3-mm observations of Saturn at low ring inclinations with our previous observations (Epstein et al., 1980) to determine a much more precise brightness temperature for Saturn's rings. Allowing for uncertainties in the optical depth and uniformity of the A and B rings and for ambiguities due to the C ring, but assuming the ring brightness to remain approximately constant with inclination, we determine a mean brightness temperature for the A and B rings of 17 ± 4 K. The portion of this brightness		

DD FORM 1473
(FACSIMILE)

UNCLASSIFIED

SECURITY CLASSIFICATION OF THIS PAGE (When Data Entered)

UNCLASSIFIED

SECURITY CLASSIFICATION OF THIS PAGE(When Data Entered)

19. KEY WORDS (Continued)

20. ABSTRACT (Continued)

attributed to ring particle thermal emission is 11 ± 5 K. The disk temperature of Saturn without the rings would be 156 ± 6 K, relative to Ulich et al.'s (1980) absolutely calibrated disk temperature for Jupiter. Assuming that the ring particles are pure water ice, a simple slab emission model leads to an estimate of typical particle sizes of ~ 0.3 m. A multiple-scattering model gives a ring particle effective isotropic single-scattering-albedo of 0.85 ± 0.05 . This albedo has been compared with theoretical Mie calculations of average albedo for various combinations of particle size distribution and refractive indices. If the maximum particle radius (~ 5 m) deduced from Voyager bistatic radar observations (Marouf et al., 1982) is correct, our results indicate either a) a particle distribution between 1 cm and several meters radius of the form r^{-s} with $3.3 < s < 3.6$, or b) a material absorption coefficient between 3 and 10 times lower than that of pure water ice Ih at 85 K, or both. Merely decreasing the density of the ice Ih particles by increasing their porosity will not produce the observed particle albedo. Our low ring brightness temperature allows us to put an upper limit on the ring particle silicate content of $\sim 10\%$ by mass if the rocky material is uniformly distributed; however, there could be considerably more silicate material if it is segregated from the icy material.

UNCLASSIFIED

SECURITY CLASSIFICATION OF THIS PAGE(When Data Entered)

PREFACE

Ms. Erika Schneider and Ms. Marion Legg provided extensive observing, data reduction, and computational assistance for this report. The work of Jeffrey N. Cuzzi was supported by the Planetary Astronomy Office of NASA through RTOP No. 196-41-67. The work of Eugene E. Epstein was supported by U.S. Air Force Contract FO4701-80-C-0081 and that of Michael A. Janssen was supported by NASA Contract NAS7-100 at JPL. Prof. Duane O. Muhleman provided a most useful critique of the manuscript.

Accession For		
NTIS GRA&I	<input checked="" type="checkbox"/>	
DTIC TAB	<input type="checkbox"/>	
Unannounced	<input type="checkbox"/>	
Justification		
By		
Distribution /		
Availability Codes		
Availability/or		
Dist	Special	
A-1		



CONTENTS

PREFACE.....	1
I. INTRODUCTION.....	9
II. OBSERVATIONS AND RESULTS.....	9
III. ANALYSIS.....	12
IV. INTERPRETATION.....	15
A. "Thin Slice of Swiss Cheese" Model.....	16
B. Multiple-Scattering Model.....	17
C. Caveat.....	22
V. DISCUSSION.....	23
REFERENCES.....	27

FIGURES

1.	Comparison of the Observed Saturn/Jupiter Ratios with the Simple 90-GHz Ring Model of Paper I.....	11
2.	Comparison of the Observed 90-GHz Saturn/Jupiter Ratios with the Multiple-Scattering Model.....	18
3.	Relationships Between the Isotropic Single-Scattering Albedo $\tilde{\omega}_{0, \text{isot}}$ at 3.3 mm and the Value of r_{max} for an Ensemble of Pure Water-Ice Particles with Size Distribution $n(r) = n_0 r^{-s}$, ($s = 3.0, 3.3$, and 3.6) from $r = 1$ cm to $r = r_{\text{max}}$ and with a 3.3-mm Absorption Coefficient Equal to That of Pure Water Ice Ih at 85 K ($\alpha/\alpha_{\text{nom}} = 1.0$).....	21

TABLES

I.	3-mm Yearly Mean Brightness Temperatures of Saturn and Jupiter.....	10
II.	Variation of the Particle Single-Scattering Albedo ω_0 and the Isotropic Single-Scattering Albedo $\omega_{0, \text{isot}}$ of Pure Water-Ice Ih Particles with Size Distribution $n(r) = n_0 r^{-s}$ from $r = 1$ cm to $r = r_{\text{max}}$ as a Function of s , r_{max} , and Absorption Coefficient $\alpha/\alpha_{\text{nom}}$	20

I. INTRODUCTION

As shown by Epstein et al. (1980; hereafter referred to as Paper I), single-antenna measurements of the combined signal from Saturn and its rings made over many years, as the ring inclination changes, can be used to determine separate values of the ring temperature and the disk temperature. However, two factors limited the specificity of Paper I's results: the large errors of the laboratory measurements of the absorption coefficient of water ice (a likely major constituent of the ring particles), and the large error of the derived ring brightness temperature because of the lack of observations at small ring inclinations. This paper utilizes new laboratory ice measurements (Mishima et al., 1983) and low-inclination observations to derive more accurate ring properties.

II. OBSERVATIONS AND RESULTS

Observations at low ring inclinations were made at 90 GHz (3.3 mm) with the Aerospace 4.6-m radio telescope, as described in Paper I, using the "FIVE" procedure. The proximity on the sky of Saturn and the reference source, Jupiter, permitted one improvement over the previous observing procedures: measurements of Saturn and Jupiter were interspersed every hour or so, instead of on a time scale of many hours or days. This fact made the system calibration and atmospheric attenuation factors for the measurements of the two planets even more uniform than previously, thus assuring the accuracy of the resulting Saturn/Jupiter ratios. Calibration and data reduction procedures were also as before. The new ratios are listed and displayed in Table I and Fig. 1, respectively, along with the ratios obtained previously.

TABLE I

3.3-mm YEARLY MEAN BRIGHTNESS TEMPERATURES OF SATURN AND JUPITER

Saturn			$\frac{(T_B) \text{ Saturn}}{(T_B) \text{ Jupiter}}$		Jupiter			
Year	Number of sets	Std. err. of mean (°K)	(T_B) (°K)	(B) (deg)	(T_B) (°K)	Std. err. of mean (°K)	Number of sets	
1965, 1967 1968	11	5	179	8.0	0.87 ± 0.05	206	9	5
1969	10	3	176	16.2	0.87 ± 0.02	203	2	8
1970	7	4	165	20.3	0.88 ± 0.02	188	3	6
1971	5	8	190	23.8	0.96 ± 0.04	197	2	13
1972	8	5	181	25.8	0.99 ± 0.03	184	2	7
1973	8	5	180	26.4	0.95 ± 0.03	188	2	9
1974	7	4	173	26.6	0.90 ± 0.03	192	2	5
1976	6	3	163	19.9	0.88 ± 0.03	185	5	5
1977	3	4	169	13.3	0.85 ± 0.03	200	4	3
1979	3	3	159	-7.1	0.89 ± 0.02	178	2	3
1979/80	3	2	160	+1.7	0.88 ± 0.01	183	1	3
1980	3	2	159	-0.8	0.88 ± 0.02	180	2	3

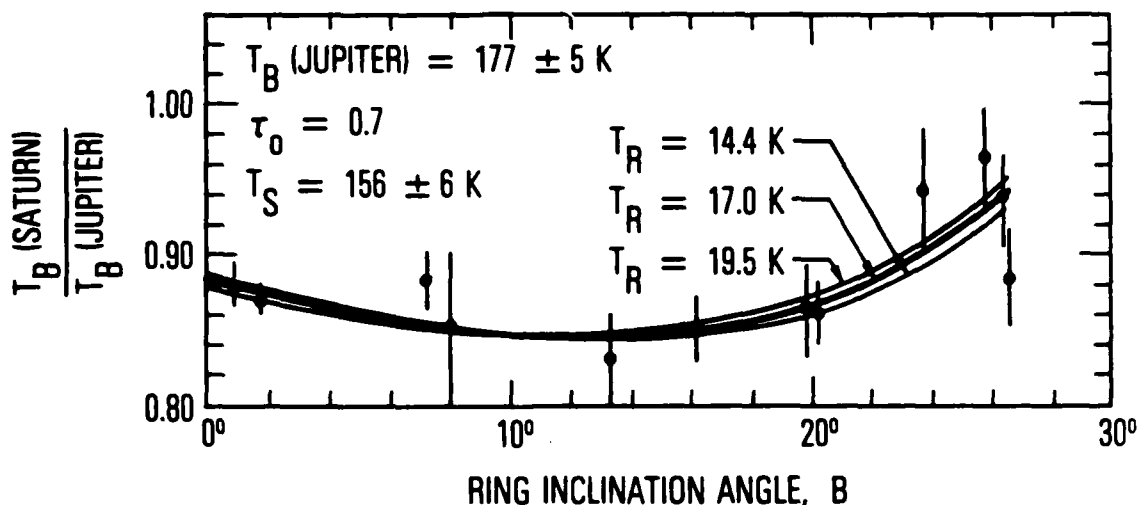


Fig. 1 Comparison of the observed Saturn/Jupiter ratios with the simple 90-GHz ring model of Paper I. The ratios here are slightly lower than those in Table I; the correction for the size of Saturn's disk has been removed from the ratios because the model convolves the image of Saturn and its rings with the Aerospace antenna pattern. The heavy curve corresponds to the simultaneous least-squares best-fit to the data of the ring brightness temperature T_R and the zero-inclination-angle intercept of the Saturn/Jupiter ratio. The thin curves indicate the 1-sigma limits to T_R . Utilizing the absolutely calibrated Jupiter brightness temperature indicated (Ulich *et al.*, 1980) leads to the Saturn disk brightness temperature T_S indicated.

III. ANALYSIS

As in Paper I, the ring brightness temperature has been derived by comparing the data with the variation with inclination of the total flux from the planet and rings predicted by a simple model with uniformly bright A and B rings (see Figs. 3 and 4 of Paper I). This model assumes that the A and B ring brightnesses (T_R) are equal, uniform, and constant with inclination angle B , and further, that the C ring is invisible. The disk of Saturn is assumed to be uniformly bright (T_S) except where the rings cross in front of the disk, in which case the brightness is the sum of the ring brightness plus that of the disk obscured by the rings ($T_R + T_S \exp[-\tau_0/\sin(B)]$), where the normal-to-the-ring optical depth τ_0 is also taken to be uniform across the rings and equal to 0.7. The free parameters of this model are the brightness temperatures of the rings (T_R) and the disk (T_S), and are determined in a simultaneous least-squares fit of the data to the model variation of total flux with ring inclination. Taking the absolutely-calibrated 86-GHz Jovian disk temperature and its 1-sigma uncertainty $T_J = 177 \pm 5$ K (Ulich *et al.*, 1980; we multiplied their value by 0.988 to convert it to the Jovian dimensions used in Paper I and we assumed that there is no change in temperature between 86 and 90 GHz), we obtain

$$T_R = 17 \pm 2.5 \text{ K}$$

$$T_S = 156 \pm 6 \text{ K.}$$

The errors are formal 1-sigma errors from the least squares fitting procedure, and include the above calibration error for the flux scale. Both values scale directly if a different flux scale is chosen. Figure 1 shows a

comparison of the data with the model result for the best-fit disk and ring temperatures (heavy curve). The light curves show the model results obtained using the 1-sigma limits on T_R and the best fitting T_S for each case. As predicted in Paper I, the addition of the low-inclination points greatly reduces the uncertainties in the derived values of T_R and T_S ; e.g., the uncertainty in T_R has been reduced from 8 to 2.5 K, while T_S is essentially directly measured by these points.

[Muhleman and Berge (1984) derived $T_R = 13 \pm 6$ K from 2.7-mm interferometry in October 1981, which agrees with our result, and $T_R = 32 \pm 4$ K from interferometry in June 1983; instrumental problems affect both results and are the cause of the discrepancy (Muhleman, 1983).]

While this model is certainly oversimplified, it was shown in Paper I that it is capable of considerable generalization. First, the model is insensitive to the actual distribution of brightness within the rings. By solving for T_R under the respective assumptions that only the A or B rings contribute to the emission, it was shown that the product of T_R times the area of the contributing ring was within 10 percent of that for the case of uniformly bright A and B rings. Hence T_R can be considered a good approximation to a mean (area averaged) ring brightness temperature. Secondly, varying the normal optical depth from 0.4 to 1.0 resulted in a total variation of only 1.5 K in T_R , so that the result is insensitive to the ring optical depth.

The effect of the C ring was neglected in Paper I because of its small area and low optical depth. We reexamined this assumption because of the much smaller error on our present result for the ring brightness temperature, and in light of a better understanding of the properties of the C ring from Voyager results. Tyler et al. (1983) find that the extinction of the C ring

is about 0.2 at 3.6-cm wavelength from 1.22 Saturn radii to the inner edge of the B ring. This extinction value must be divided by 2 to obtain the optical depth appropriate for the present radiative transfer problem, because strongly forward-scattered radiation still contributes to the brightness of the disk seen through the rings (Cuzzi and Pollack, 1978, and Cuzzi et al., 1980). Comparison of the 3.6-cm optical depth with that at visual wavelengths shows little variation beyond this effect (Cuzzi et al., 1984). Assuming that the 3-mm optical depth is the same as that at 3.6 cm, we included the C ring in our model with a normal optical depth of 0.1 and a brightness temperature modelled as

$$T_R^{(C)} = \epsilon T_0 (1 - \exp[-0.1/\sin|B|])$$

where $T_0^{(C)}$ is the physical temperature of the C ring particles and ϵ their average emissivity. Emission from the region of the disk obscured by the C ring is of course reduced by the factor $\exp[-0.1/\sin|B|]$.

The C ring brightness temperature is fully determined if $T_0^{(C)}$ and ϵ are chosen. Taking $T_0^{(C)} = 100$ K and letting ϵ take the extreme values of 0 and 1, we again solved for a uniform T_R for the combined A and B rings, obtaining $T_R = 19.2$ and 13.9 K respectively. The goodness of fit by a chi-square measure does not vary significantly, and in all cases is fully consistent with the measurement errors. If we consider that all values for ϵ are equally likely, then the result for T_R originally obtained is essentially unchanged, while the uncertainty introduced by our lack of knowledge about the emissivity of the C ring is comparable to that of our original formal error for T_R . Conversely, the present results tell us nothing new about the C ring.

We conclude that the derived ring brightness temperature represents a mean brightness temperature for the A and B rings which is valid for a wide range of possible models for the entire ring system. Taking the above sources of uncertainty into account, we estimate that the mean ring brightness temperature is

$$\bar{T}_R = 17 \pm 4 \text{ K.}$$

This result presumes that the ring brightness temperature remains constant as the ring inclination varies. However, the ring brightness will change inasmuch as both the physical temperature of the ring particles and their scattering properties will depend upon inclination. It is apparent from Fig. 4 of Paper I that the model is most sensitive to T_R for $B \gtrsim 10$ deg and is not sensitive to T_R at low inclinations (where the largest brightness variations would be expected to occur) so that the present result is weighted toward the larger inclinations. A more detailed model is needed to make this consideration more quantitative - such a model is described in Sec. IV. B below and leads to a ring brightness temperature averaged over radius and inclination which is consistent with the above result.

IV. INTERPRETATION

We use the same two methods outlined in Paper I to obtain improved limits on particle and ring properties on the assumption that the particles are pure water ice.

A. "Thin Slice of Swiss Cheese" Model

Diffuse scattering of the planet's thermal emission produces a radially dependent component of the total ring brightness of average magnitude 6 ± 3 K (Paper I). Subtracting out this scattered emission leaves

$$T_t = 11 \pm 5 \text{ K.}$$

We regard this latter component as representing the intrinsic thermal emission from the rings; it is now a definite result rather than the upper limit obtained in Paper I. This result allows us to estimate the mean rather than the limiting properties of the rings. For example, consider the simple slab (or "thin slice of Swiss cheese") model (Paper I). For this model the rings are regarded simply as a uniform rough slab (but with holes in it to represent the spaces between particles) of thickness r , normal-to-the-ring, optical depth τ_0 , and physical temperature T_0 ; the thermal component T_t of the brightness temperature is given approximately by

$$T_t = \alpha(1 - e^{-\tau_0 \csc|B|})T_0 \quad (1)$$

where α is the wavelength-dependent absorption coefficient of the ring material. The exponential term accounts for the open area between particles and is a good approximation for a monolayer if B is not too small (Cuzzie and Pollack, 1978). We take, as in Paper I, $\tau_0 \csc|B| = 0.7 \csc 20^\circ \approx 2$ and $T_0 = 85 \text{ K}$ [derived from $22.7\text{-}\mu\text{m}$ ground-based observations at $B' = 16$ and 26° (see Nolt et al., 1978)]. From extensive new laboratory measurements of pure water ice, Mishima, Klug, and Whalley (1983) have derived at 3.3 mm and 85 K , an absorption coefficient $\alpha = (4.8 \pm 1.0) \times 10^{-3} \text{ cm}^{-1}$. (This value is 1.5 times larger than the value adopted in Paper I.) We then obtain

$$r = 30 \pm 13 \text{ cm}$$

for the thickness of a simple ice-slab model ring. Because T_0 decreases somewhat as $|B|$ decreases, this value of r is possibly somewhat low. A more detailed model is discussed next.

B. Multiple-Scattering Model

This method employs a numerical radiative transfer model in which the A, B, and C rings are represented by scattering/emitting layers of finite optical depth. The exact particle single-scattering albedo ($\tilde{\omega}_0$) and phase function are determined by Mie scattering calculations, assuming only the particle size distribution and refractive indices $n_r + in_i = n_r + (\frac{\lambda}{4\pi} \alpha)i$. Because of the ensuing high particle albedos, the net brightness of the rings results from a combination of ring thermal emission and diffuse reflection of planetary thermal emission. This model is described in Paper I and in more detail by Cuzzi et al. (1980); it is compared with the observations in Fig. 2. The heavy curve corresponds to the simultaneous least-squares best fit to the data of the zero-inclination intercept of the Saturn system/Jupiter ratio and $\tilde{\omega}_{0,\text{isot}}$, which is a scaled effective albedo for isotropic scattering obtained [by similarity relations (Paper I and Irvine, 1975)] from the real albedo and a (highly forward-scattering) phase function. The thin curves correspond to the 1-sigma limits on $\tilde{\omega}_{0,\text{isot}}$. The best-fit values of $\tilde{\omega}_{0,\text{isot}}$ and T_S are

$$\tilde{\omega}_{0,\text{isot}} = 0.85 \pm 0.05$$

$$T_S = 156 \pm 6 \text{ K,}$$

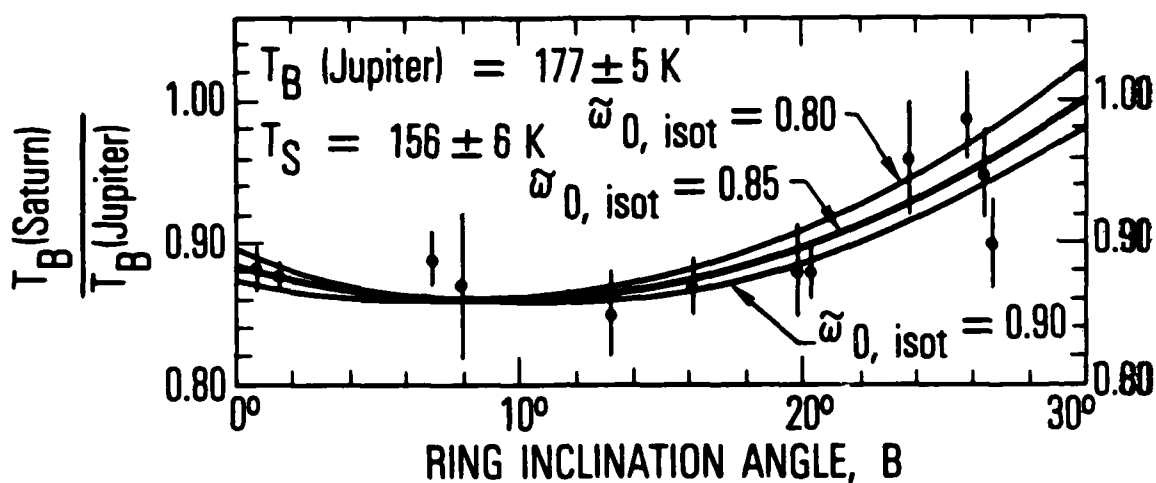


Fig. 2 Comparison of the observed 90-GHz Saturn/Jupiter ratios with the multiple-scattering model. The heavy curve corresponds to the simultaneous least-squares best-fit to the data of the equivalent isotropic single-scattering albedo $\tilde{\omega}_{0, \text{isot}}$ and the zero-inclination-angle intercept of the Saturn/Jupiter ratio. The thin curves indicate the 1-sigma limits to $\tilde{\omega}_{0, \text{isot}}$. Utilizing the absolutely calibrated Jupiter disk brightness shown (Ulich *et al.*, 1980) leads to the Saturn disk brightness temperature T_S indicated.

where the error for T_S accounts for uncertainties in the ring optical depth (which are negligible--see Paper I and Sec. III), in Jupiter's disk temperature, and in the fitting. In these calculations the ring physical temperature is assumed to vary with solar elevation angle B' , as is observed [see the discussion in Paper I and, e.g., Nolt et al. (1978)]. The inclination-averaged ring brightness temperature computed using this multiple-scattering model and $\tilde{\omega}_{0, \text{isot}} = 0.85$ is ≈ 15 K — consistent with the value of 17 ± 3 K derived from the simpler model of Sec. III which assumes the ring brightness to be independent of inclination angle.

We also investigated the possible effect on the results of the presence of "holes" in the rings. If a few percent of the ring area has an optical depth of only a few percent [as implied by analyses of Pioneer Saturn data (Esposito et al., 1980)], then blockage of the planetary emission will be less at low inclination angles than if a homogeneous ring were assumed. Such "holes" will cause our multiple scattering model to derive a spuriously low value of $\tilde{\omega}_{0, \text{isot}}$, but by an amount less than the above formal error. Thus if "holes" exist, the true value of $\tilde{\omega}_{0, \text{isot}}$ may be slightly higher than quoted above. Voyager observations, however, do not support such a large fraction of empty space (Lane et al., 1982; Esposito et al., 1983). Consequently, in this regard, our value of $\tilde{\omega}_{0, \text{isot}}$ is acceptable.

The variations of the particle single-scattering albedo $\tilde{\omega}_0$ and the isotropic single-scattering albedo $\tilde{\omega}_{0, \text{isot}}$ as a function of absorption coefficient α , assumed size distributions for the particle volume density $n(r) = n_0 r^{-s}$, and maximum particle size r_{max} (assuming $r_{\text{min}} = 1.0$ cm for all cases) are shown in Table II and Fig. 3. The tabulated values of $\tilde{\omega}_0$ and the asymmetry parameter g are obtained by averaging over the indicated particle distribution; $\tilde{\omega}_{0, \text{isot}}$ is obtained from $\tilde{\omega}_0$ and g (see Table II, Footnote c).

TABLE II

VARIATION OF THE PARTICLE SINGLE-SCATTERING ALBEDO $\tilde{\omega}_0$ AND THE ISOTROPIC SINGLE-SCATTERING ALBEDO $\tilde{\omega}_{0, \text{isot}}$ OF PURE WATER-ICE Ih PARTICLES WITH SIZE DISTRIBUTION $n(r) = n_0 r^{-s}$ FROM $r = 1 \text{ cm}$ TO $r = r_{\text{max}}$ AS A FUNCTION OF s , r_{max} , AND ABSORPTION COEFFICIENT $\alpha/\alpha_{\text{nom}}^a$

s	r_{max} (μ)	$\alpha/\alpha_{\text{nom}}^a$	$\tilde{\omega}_0^b$	$g^{b,c}$	$\tilde{\omega}_{0, \text{isot}}^{b,c}$
3.0	1.0	1.0	0.954	0.749	0.838
3.0	5.0	1.0	0.869	0.775	0.599
3.0	1.0	0.3	0.983	0.738	0.940
3.0	3.0	0.3	0.953	0.749	0.840
3.0	5.0	0.3	0.926	0.758	0.750
3.0	1.0	0.1	0.994	0.734	0.980
3.0	3.0	0.1	0.981	0.739	0.930
3.0	5.0	0.1	0.967	0.744	0.880
3.3	1.0	1.0	0.968	0.737	0.888
3.3	3.0	1.0	0.931	0.747	0.780
3.3	5.0	1.0	0.906	0.755	0.700
3.3	1.0	0.3	0.988	0.729	0.960
3.3	3.0	0.3	0.968	0.736	0.890
3.3	5.0	0.3	0.949	0.743	0.830
3.3	1.0	0.1	0.996	0.726	0.990
3.3	3.0	0.1	0.987	0.730	0.950
3.3	5.0	0.1	0.978	0.733	0.920
3.6	1.0	1.0	0.977	0.727	0.921
3.6	3.0	1.0	0.954	0.733	0.850
3.6	5.0	1.0	0.937	0.738	0.796

^a $\alpha_{\text{nom}} = 4.8 \times 10^{-3} \text{ cm}^{-1}$ at 3.3 μm (Mishima *et al.*, 1983).

^b These values are obtained by averaging over the indicated particle size distribution.

^c The isotropic single-scattering albedo $\tilde{\omega}_{0, \text{isot}} = \tilde{\omega}_0(1 - g)/(1 - \tilde{\omega}_0 g)$,

where the asymmetry parameter $g = 2 \pi \int_{-1}^1 \cos \theta p(\theta) \sin \theta d\theta$ (see Paper I).

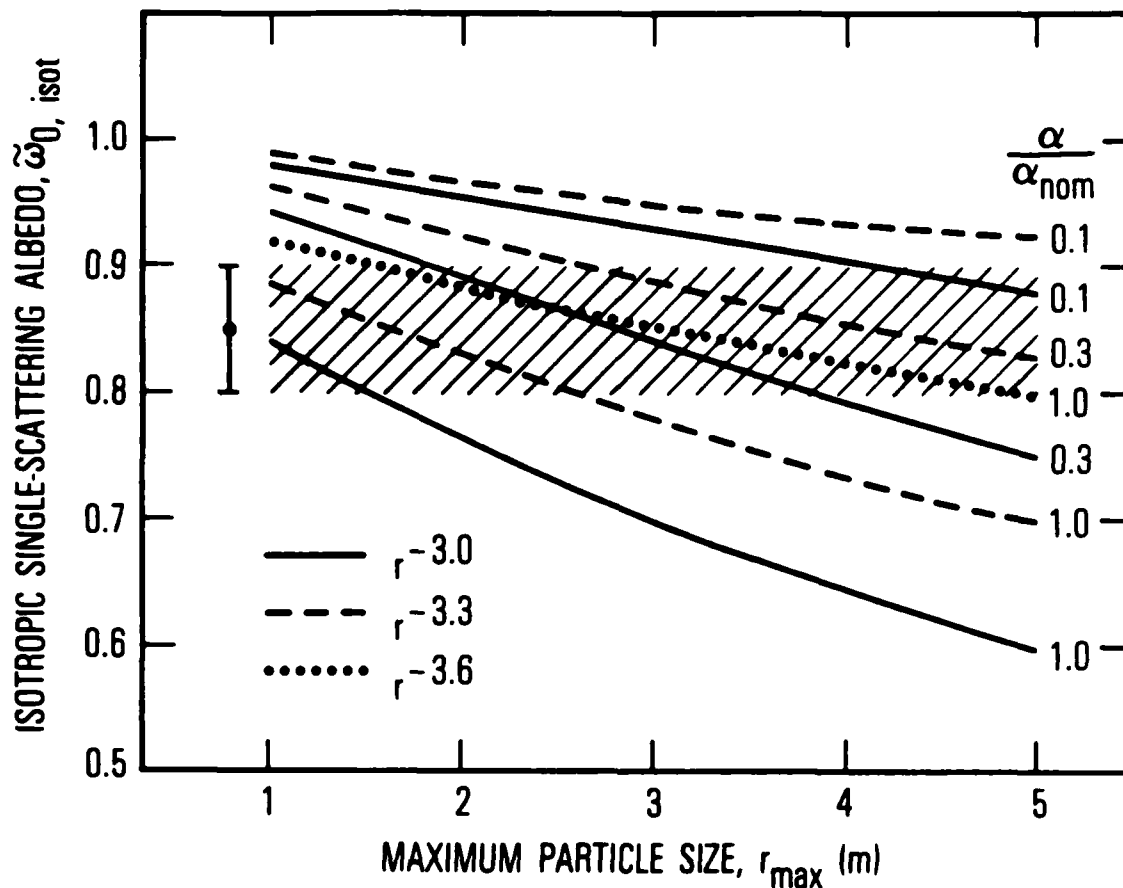


Fig. 3 Relationships between the isotropic single-scattering albedo $\tilde{\omega}_{0, \text{isot}}$ at 3.3 mm and the value of r_{max} for an ensemble of pure water-ice particles with size distribution $n(r) = n_0 r^{-s}$, ($s = 3.0, 3.3$, and 3.6) from $r = 1$ cm to $r = r_{\text{max}}$ and with a 3.3-mm absorption coefficient equal to that of pure water ice Ih at 85 K ($\alpha/\alpha_{\text{nom}} = 1.0$). Also shown are the relationships for particles with absorption coefficients 0.1 and 0.3 that of pure water ice ($\alpha/\alpha_{\text{nom}} = 0.1$ and 0.3). The best-fit value of $\tilde{\omega}_{0, \text{isot}} = 0.85 \pm 0.05$, as derived from comparison of the 3.3-mm observations with the multiple-scattering model, is indicated by the cross-hatching.

The observed absorption coefficient α is normalized by the nominal value at 3.3 mm for pure water ice Ih at 85 K of $\alpha_{\text{nom}} = 4.8 \times 10^{-3} \text{ cm}^{-1}$ (Mishima et al., 1983). Values used for the slope s in the power law are 3.0, 3.3, and 3.6; this range is consistent with ground-based radar observations (Cuzzi and Pollack, 1978). Further, Voyager results indicate that the slope s is between 3.2 and 3.4 (Marouf et al., 1982). Marouf et al. also deduced that $r_{\text{max}} \sim 5 \text{ m}$ in most of the ring system; only in the C ring, which contributes little to the 3-mm emission, is r_{max} possibly as small as 1 m. Inspection of Fig. 3, where our result for $\tilde{\omega}_{0,\text{isot}}$ of 0.85 ± 0.05 is indicated by the cross-hatching, shows that for our result to be consistent with an r_{max} as large as 5 m, either the slope s must be ~ 3.6 , or the particle absorption coefficient α at 3 mm must be 0.1 to 0.3 of α_{nom} , or some combination of the two. A slope of 3.6 is somewhat larger than the best-fit Voyager result, but not impossibly so. Since the ring particles are unlikely to be pure water ice (Clark, 1980), or since they could contain ice in its amorphous phase, it is possible that the particles' absorption coefficient could be lower than that of pure ice Ih. The calculations displayed in Fig. 3 indicate that self-consistency between all the constraints is achieved if $r_{\text{max}} \sim 5 \text{ m}$, $s \sim 3.3$, and $\alpha \sim 0.5 \alpha_{\text{nom}}$.

C. Caveat

If interparticle shadowing causes particles deep within the ring layer to be physically cooler than those which are unshadowed, then some of this discrepancy in α may be removed. Furthermore, we note that the Voyager size distribution refers to regions of low to moderate optical depth, whereas our measurements refer to regions of moderate to high optical depth where the exact size distribution is not as well known and may be different.

We also investigated the effect of merely decreasing the density of the ring particles. The refractive index was assumed to vary with density as predicted by the Rayleigh mixing formula, as suggested by laboratory measurements (Campbell and Ulrichs, 1969). The effect of decreasing density is thus to decrease both the real and imaginary indices of refraction. The main effect on particle scattering properties was to increase the degree of forward scattering, but not to change the albedo. Model calculations of ring temperatures showed that the fit to the brightness temperature data was not improved by such a decrease in particle density, and that implications for r_{\max} and s were not affected. Therefore, we feel that there is no evidence that the particle density is much lower than that of solid ice. However, these data cannot rule out the presence of a particle density somewhat less than unity.

V. DISCUSSION

The low brightness temperature strongly implies the presence of a low-loss dielectric and places a limit on the amount of high-loss material which can be present. In the present case we may estimate an upper limit to the rock/ice ratio within the rings. The absorption coefficient of chondritic type material at 3.3 mm ranges upward from approximately 0.8 cm^{-1} (Campbell and Ulrichs, 1969). At lower densities (e.g., loose powders or dispersed particles), the absorption coefficient of a mixture is approximately proportional to the fraction of the absorber. Hence, from Eq. (1), distributed material of total quantity equivalent to a slab of 2 mm thickness would produce a 3.3-mm brightness temperature of 15 K for $T_0 = 85 \text{ K}$. This is the largest quantity of such rocky material which can be present, if uniformly and finely divided. On the other hand, the minimum quantity of ice required in

order to scatter radar at X- and S-band is a monolayer of particles of radius $\gtrsim 6$ cm (Cuzzi and Pollack, 1978). Therefore, allowing for a rock density of 2.4 g/cm^3 , the rock/ice ratio must be less than about 10% if the materials are uniformly mixed, consistent with radar observations (Cuzzi and Pollack, 1978). A more stringent limit may be placed using our derived values of $r_{\text{max}} \sim 5$ m, $s \sim 3.3$ and $\alpha \sim 0.5\alpha_{\text{nom}}$ (i.e., the observed absorption coefficient α is about half the nominal absorption coefficient of ice). If the rocky material were a minor, uniformly distributed fraction and the dominant icy material had an absorption coefficient of zero, there could be no more than $(\text{observed } \alpha)/(\text{rock } \alpha) \sim 2.4 \times 10^{-3}/0.8 \sim 3 \times 10^{-3}$ by volume of any rocky or carbonaceous absorber.

This result argues strongly for some sort of chemical differentiation having taken place within the rings. Several current theories for the origin of the rings involve condensation more or less in situ from a cloud of solar composition around Saturn (e.g., Pollack, 1975; Cameron, 1977). Without differentiation, and assuming that all the H_2O (but not necessarily all the NH_3 or CH_4) is retained, then the ratio of rock/ice would be about 50% (Consolmagno and Lewis, 1977). The lowest-density Saturnian satellites seem to have about a 20% rock/ice ratio (Smith et al., 1982). A ratio of 10% or less would seem to imply that an even more significant loss of rock has taken place in the rings than in the satellites relative to the original solar nebula.

However, it is not necessary to physically remove the rock completely from the rings to achieve the present result. Rather, the rock need only be hidden from view at microwave frequencies. For example, we may consider a bimodal distribution of material within the rings such that the rock is contained in a small number of relatively large particles, while the ice is more

broadly distributed, possibly in different particles. If the rock particles are a few meters or larger in diameter, then they may contain an effectively unlimited mass relative to the ice without contributing significantly to the thermal emission because their net cross-sectional area remains small.

Such a situation could arise as follows: Differential condensation of a solar composition cloud around Saturn could have occurred according to the model of Consolmagno and Lewis (1977), leaving initially a swarm of small rocky bodies of meter-size and larger. Subsequent cooling of the nebula would result in further condensation of volatiles, producing an ice coating on these bodies. As they are within Roche's limit (i.e., in the vicinity of the rings), these "moonlets" may not have accreted further into larger bodies, but may remain more or less in place restricted in size ($\ll 1$ km) at the present. Meanwhile, repeated weak collisions among these bodies have chipped the ice from their surfaces. These ice particles, with sizes of centimeters to meters, produce most of the visible surface of the rings. The surface area of the parent objects is much less than the surface area of the "visible" ring particles. Furthermore, their total surface area is far less than if uniformly dispersed into small particles. This model requires only that "local" differentiation has taken place. Alternatively, of course, differentiation processes on larger scales may have been active to segregate the rocky material or even to remove this material entirely from the vicinity of the rings, e.g., through viscous drag on the initial condensation of rocky moonlets by the as-yet-uncondensed volatile component (Pollack, 1975). The anomalously low densities of Saturn's satellites measured by Voyager could also be indicative of such a process. Preliminary photometry of Voyager imaging results points to variations of particle albedo in the rings from ~ 0.3 in the C ring to ~ 0.6 in the A and B rings; also, closer

inspection shows comparable variations in albedo even on scales of 50 - 100 km in the B ring (Cuzzi et al., 1984). This inhomogeneity is supportive of our suggestions above.

REFERENCES

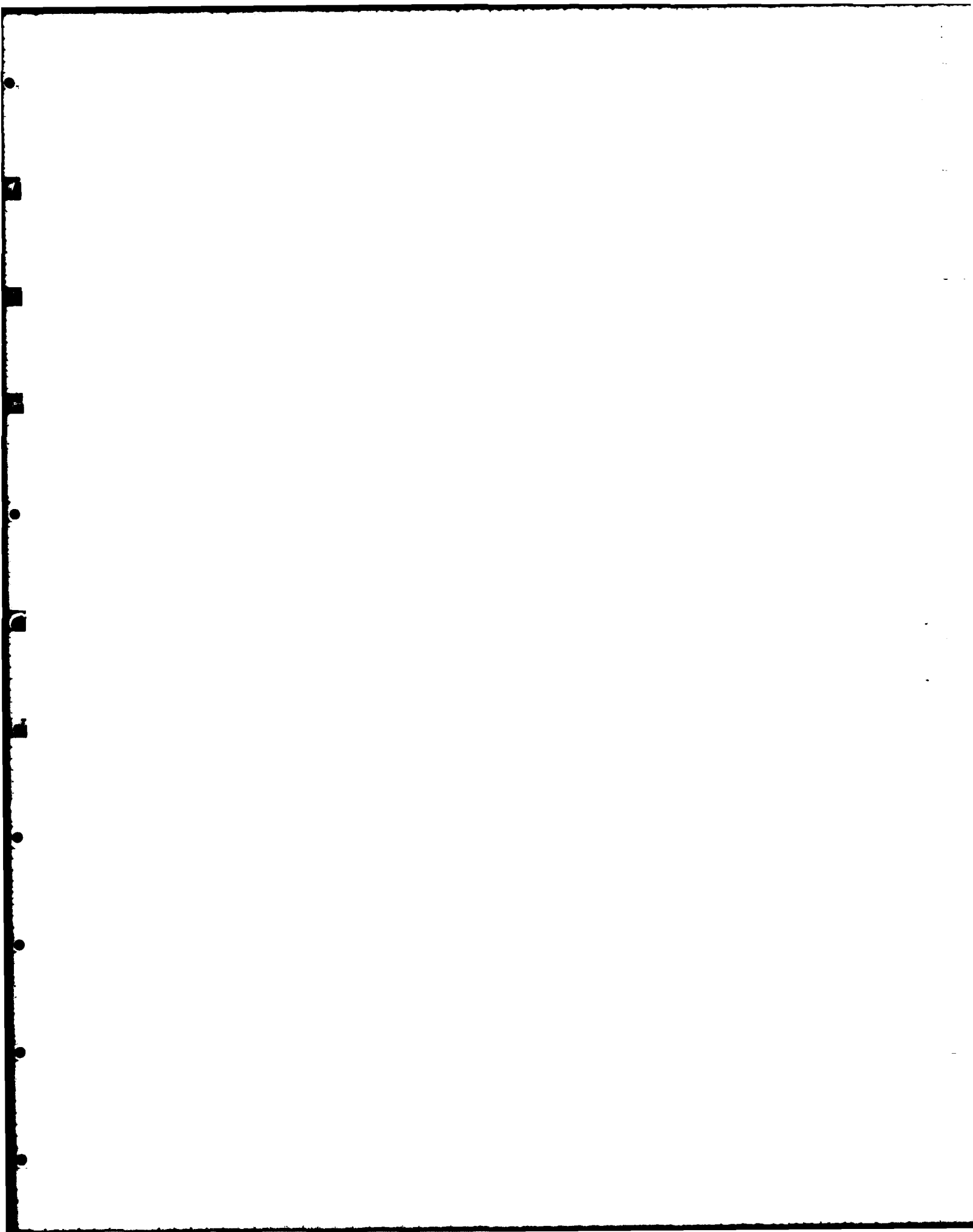
- Cameron, A. G. W. (1977). Formation of the outer planets and satellites. In Planetary Satellites (J. Burns, ed.), 463-471. University of Arizona Press, Tucson.
- Campbell, M. J., and Ulrichs, J. (1969). Electrical properties of rocks and their significance for lunar radar observations. *J. Geophys. Res.* 74, 5867-5881.
- Clark, R. N. (1980). Ganymede, Europa, Callisto, and Saturn's rings: Compositional analysis from reflectance spectroscopy. *Icarus* 44, 388-409.
- Consolmagno, G. J., and Lewis, J. S. (1977). Preliminary thermal history models of icy satellites. In Planetary Satellites (J. Burns, ed.), 492-500. University of Arizona Press, Tucson.
- Cuzzi, J. N., Lissauer, J. J., Esposito, L. W., Holberg, J. B., Marouf, E. A., Tyler, G. L., and Boischot, A. (1984). Saturn's rings: Properties and processes. In Planetary Rings (R. Greenberg and A. Brahic, eds.), xxx-xxx. University of Arizona Press, Tucson.
- Cuzzi, J. N., and Pollack, J. B. (1978). Saturn's rings: Particle composition and size distribution as constrained by microwave observations. I. Radar observations. *Icarus* 33, 233-262.
- Cuzzi, J. N., Pollack, J. B., and Summers, A. L. (1980). Saturn's rings: particle composition and size distribution as constrained by observations at microwave wavelengths. II. Radio interferometric observations. *Icarus*, 44, 683-705.
- Epstein, E. E., Janssen, M. A., Cuzzi, J. N., Fogarty, W. G., and Mottmann, J. (1980). Saturn's rings: 3-mm observations and derived properties. *Icarus* 41, 103-118.

- Esposito, L. W., Dilley, J. P., and Fountain, J. W. (1980). Photometry and polarimetry of Saturn's rings from Pioneer Saturn. *J. Geophys. Res.* 85, 5948-5956.
- Esposito, L. W., O'Callaghan, M., and West, R. A. (1983). The structure of Saturn's rings: Implications from the Voyager stellar occultation. *Icarus*, 56, 439-452.
- Irvine, W. M. (1975). Multiple scattering in planetary atmospheres. *Icarus* 25, 175-204.
- Lane, A. L., Hord, C. W., West, R. A., Esposito, L. W., Coffeen, D. L., Sato, M., Simmons, K. E., Pomphrey, R. B., and Morris, R. B. (1982). Photo-polarimetry from Voyager 2: preliminary results on Saturn, Titan and the rings. *Science* 215 537-543.
- Marouf, E. A., Tyler, G. L., Zebker, H. A. and Eshleman, V. R. (1982). Particle-size distributions in Saturn's rings from Voyager 1 radio occultation. *Icarus*, in press.
- Mishima, O., Klug, D. D., and Whalley, E. (1983). The far-infrared spectrum of ice Ih in the range of $8 - 25 \text{ cm}^{-1}$. Sound waves and difference bands, with application to Saturn's rings. *J. Chem. Phys.* 78, 6399-6406.
- Muhleman, D. O., and Berge, G. L. (1984). Microwave emission from Saturn's rings at $\lambda = 2.7 \text{ mm}$. In *Planetary Rings* (A. Brahic, ed.), Proceedings of IAU Colloquium No. 75, in press.
- Muhleman, D. O. (1983). Private communication.
- Nolt, I. G., Tokunaga, A., Gillett, F., and Caldwell, J. (1978). The 22.7 micron brightness temperature of Saturn's rings versus declination of the Sun. *Astrophys. J.* 219, L63-L66.
- Pollack, J. B. (1975). The rings of Saturn. *Space Sci. Rev.* 18, 3-93.

Smith, B. A., Soderblom, L., Batson, R., Bridges, P., Inge, J., Masursky, H., Shoemaker, E., Beebe, R., Boyce, J., Briggs, G., Bunker, A., Collins, S. A., Hansen, C. J., Johnson, T. V., Mitchell, J. L., Terrile, R. J., Cook, A. F., II, Cuzzi, J., Pollack, J. B., Danielson, G. E., Ingersoll, A. P., Davies, M. E., Hunt, G. E., Morrison, D., Owen, T., Sagan, C., Veverka, J., Strom, R., and Suomi, V. E. (1982). A new look at the Saturn system: the Voyager 2 images. *Science* 215, 504-537.

Tyler, G. L., Marouf, E. A., Simpson, R. A., Zebker, H. A., and Eshleman, V. R. (1983). The microwave opacity of Saturn's rings at wavelengths of 3.6 and 13 cm from Voyager 1 radio occultation. *Icarus* 54, 160-188.

Ulich, B. L., Davis, J. H., Rhodes, P. J., and Hollis, J. M. (1980). Absolute brightness temperature measurements at 3.5 mm wavelength. *IEEE Trans. Antennas Propagat.* AP-28, 367-376.



LABORATORY OPERATIONS

The Laboratory Operations of The Aerospace Corporation is conducting experimental and theoretical investigations necessary for the evaluation and application of scientific advances to new military space systems. Versatility and flexibility have been developed to a high degree by the laboratory personnel in dealing with the many problems encountered in the nation's rapidly developing space systems. Expertise in the latest scientific developments is vital to the accomplishment of tasks related to these problems. The laboratories that contribute to this research are:

Aerophysics Laboratory: Launch vehicle and reentry aerodynamics and heat transfer, propulsion chemistry and fluid mechanics, structural mechanics, flight dynamics; high-temperature thermomechanics, gas kinetics and radiation; research in environmental chemistry and contamination; cw and pulsed chemical laser development including chemical kinetics, spectroscopy, optical resonators and beam pointing, atmospheric propagation, laser effects and countermeasures.

Chemistry and Physics Laboratory: Atmospheric chemical reactions, atmospheric optics, light scattering, state-specific chemical reactions and radiation transport in rocket plumes, applied laser spectroscopy, laser chemistry, battery electrochemistry, space vacuum and radiation effects on materials, lubrication and surface phenomena, thermionic emission, photosensitive materials and detectors, atomic frequency standards, and bioenvironmental research and monitoring.

Electronics Research Laboratory: Microelectronics, GaAs low-noise and power devices, semiconductor lasers, electromagnetic and optical propagation phenomena, quantum electronics, laser communications, lidar, and electro-optics; communication sciences, applied electronics, semiconductor crystal and device physics, radiometric imaging; millimeter-wave and microwave technology.

Information Sciences Research Office: Program verification, program translation, performance-sensitive system design, distributed architectures for spaceborne computers, fault-tolerant computer systems, artificial intelligence, and microelectronics applications.

Materials Sciences Laboratory: Development of new materials: metal matrix composites, polymers, and new forms of carbon; component failure analysis and reliability; fracture mechanics and stress corrosion; evaluation of materials in space environment; materials performance in space transportation systems; analysis of systems vulnerability and survivability in enemy-induced environments.

Space Sciences Laboratory: Atmospheric and ionospheric physics, radiation from the atmosphere, density and composition of the upper atmosphere, aurorae and airglow; magnetospheric physics, cosmic rays, generation and propagation of plasma waves in the magnetosphere; solar physics, infrared astronomy; the effects of nuclear explosions, magnetic storms, and solar activity on the earth's atmosphere, ionosphere, and magnetosphere; the effects of optical, electromagnetic, and particulate radiations in space on space systems.

. . .

END

FILMED

9-34

END